J. Plasma Physics (2014), *vol.* 80, *part* 3, *pp.* 417–423. © Cambridge University Press 2013
doi:10.1017/S0022377813001384

On error field penetration processes in magnetic island mode locking

H. H. Wang[1], Z. X. Wang[1]† and X. G. Wang[2]

[1]MOE Key Laboratory of Materials Modification by Beams, School of Physics and Optoelectronic Engineering, Dalian University of Technology, Dalian 116024, China
[2]School of Physics, Peking University, Beijing 100871, China

(Received 1 September 2013; revised 14 October 2013; accepted 21 October 2013; first published online 13 December 2013)

Error field penetration processes in magnetic island mode locking with the time-varying and fixed boundary perturbations are investigated numerically by using a two-dimensional resistive magnetohydrodynamic model in slab geometry. The evolution of various poloidal torques on the rational surface in the processes is analyzed in detail. In particular, three different states with the fixed boundary perturbations, viz. below the threshold (nearly locked regime), on the threshold (just locked regime), and above the threshold (strongly locked regime), are discussed and compared with the physical processes of the Rutherford regime.

1. Introduction

Theoretically, the magnetic field is designed to be well embedded in toroidal plasmas. However, mismatches in the processes of winding, connecting, and assembling the magnetic coils and other parts, and the ferromagnetic materials of the vacuum chamber always produce the so-called error fields, whose intensity is about 10^{-3} to 10^{-5} of toroidal magnetic field (Callen 2011). Error fields slow down the plasma flow velocity so as to induce the locked modes that degrade the density and temperature confinements and even lead to major disruption.

Error field-locked modes have motivated extensive investigations in experiments, theoretical analyses, and numerical simulations since the early 1990s. Relevant experimental investigations in various tokamak devices, such as COMPASS (Hender et al. 1992; Buttery et al. 1999), JET (Fishpool and Haynes 1994; Buttery et al. 1999; Buttery et al. 2000; Lazzaro et al. 2002), TEXTOR (Wolf et al. 2005), DIII-D (Buttery et al. 1999), C-Mod (Wolfe et al. 2005), J-TEXT (Hu et al. 2012; Jin et al. 2013), etc., have been carried out by applying resonant perturbation magnetic fields (i.e. RMPs) under different conditions, for example, ohmic heating (Hu et al. 2012; Jin et al. 2013), neutral beam injection (NBI) (Fishpool and Haynes 1994; Lazzaro et al. 2002), and other auxiliary heating techniques (Wolfe et al. 2005). All these experiments provided a primary concern for theoretical and numerical researches. Recent theoretical investigations have covered from one- to three-dimensional results in the frames of magnetohydrodynamic (MHD), two-fluid, and kinetic models (Jensen and Leonard 1991; Boozer 1996; Ma et al. 1996; Wang and Bhattacharjee 1997; Waelbroeck et al. 2012). Nonetheless, majority of the works are on the linear analysis. In the numerical aspect, the simulation investigations started in the early 1990s (Parker

† Email address for correspondence: zxwang@dlut.edu.cn

https://doi.org/10.1017/S0022377813001384 Published online by Cambridge University Press

1992), and have became an important tool to predict the real experiments recently (Fitzpatrick 2003; Zha et al. 2005; Yu et al. 2008; Yu et al. 2009; Xu et al. 2011; Liu et al. 2012). However, most of the previous studies have focused on seeking the locked mode thresholds, and the evolution process in different regimes still needs to be further understood. One of such prominent problems is the Rutherford regime of error field penetration. The Rutherford regime originated from the classic nonlinear tearing mode theory (Rutherford 1973). Recently, the Rutherford island evolution equation has been employed in the neo-classic tearing mode analysis with the effects of bootstrap current, poloidal current, and externally applied current drive terms (Mirnov et al. 1999; Hender et al. 2007). The Rutherford model was also applied in error field-locked modes in 1990 (Nave and Wesson 1990), and subsequently series of relevant theoretical investigations were conducted (Fitzpatrick 1993; Wang and Bhattacharjee 1997; Fitzpatrick 1998). However, direct simulations of the error field mode locking process in the Rutherford regime are still needed to further understand the process.

In this study, we investigate the error field penetration processes in the Rutherford regime mode locking. Both time-varying and fixed boundary perturbations are applied to explore island evolutions. The time evolutions of poloidal torques and poloidal flow velocity on the rational surfaces are presented. Besides, three initial states of different mode locking regimes are discussed in detail. Section 2 describes the model and equilibrium, and Sec 3 presents numerical results with time-varying and fixed boundary conditions. Finally, conclusions are given in Sec 4.

2. Model and equilibrium

In this work, we employ a two-dimensional resistive MHD model in slab geometry (Wang et al. 2007; Wang et al. 2008), where a sheet pinch layer of current flowing along the z-direction is applied. The equations are given as follows:

$$\frac{\partial p}{\partial t} = -\boldsymbol{u}\cdot\nabla p - \gamma p\nabla\cdot\boldsymbol{u}, \tag{1}$$

$$\rho\frac{\partial \boldsymbol{u}}{\partial t} = -\boldsymbol{u}\cdot\nabla\boldsymbol{u} - \nabla\left[p + B^2/2\right] + \mu\nabla^2\boldsymbol{u}, \tag{2}$$

$$\frac{\partial \psi}{\partial t} = -\boldsymbol{u}\cdot\nabla\psi + \eta\nabla^2\psi. \tag{3}$$

Here the density ρ is constant, p denotes the pressure, and $\boldsymbol{u}$ denotes the plasma flow velocity. The magnetic flux function, ψ, is denoted by $\mathbf{B} = \nabla\psi\times\hat{z}$, where $\mathbf{B}$ is the magnetic field, η and μ are plasma resistivity and viscosity, respectively, and γ is the adiabatic coefficient. All the quantities are normalized as $x\to x/a$, $t\to t/(a/V_A)$, $p\to p/\rho V_A^2$, $\boldsymbol{u}\to\boldsymbol{u}/V_A$, $\psi\to\psi/(aB_0)$, $\mu\to\mu/(a\rho V_A)$, $\eta\to\eta/(a\mu_0 V_A)$, where $V_A = B_0/\sqrt{\mu_0\rho}$ and a are the poloidal Alfvén velocity and the tokamak plasma minor radius, respectively. The initial equilibrium and boundary conditions are employed as in Fitzpatrick (2003).

3. Numerical results and analysis

The code has been benchmarked in an earlier paper (Wang et al. 2013) according to the first typical example reported in Fitzpatrick (2003). In the following, we first investigate the mode locking process with the time-varying boundary perturbations in the Rutherford regime, and then discuss three different initial states with fixed

https://doi.org/10.1017/S0022377813001384 Published online by Cambridge University Press

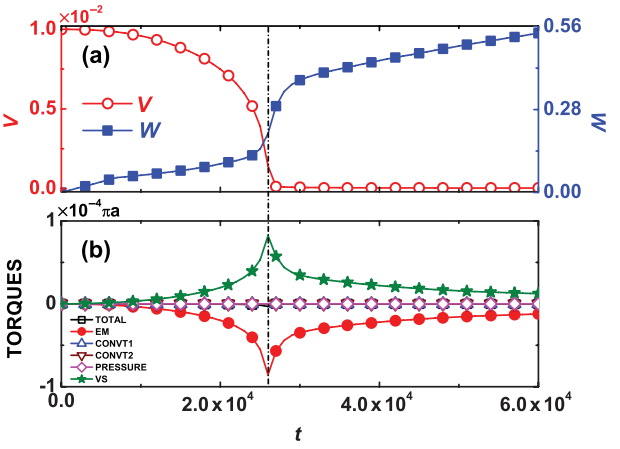


FIGURE 1. (Color online) (a) Time evolution of the azimuthally averaged poloidal velocity (AAPV),V, on the rational surface and relevant island width,W, where the island width is the length with the simulation width,$X_w = \pm 2.5$. (b) Time evolution of the decomposed averaged torque in the poloidal direction on the rational surface, EM is the electromagnetic torque ($-\nabla^2\psi\frac{\partial\psi}{\partial y}$), CONVT1 is the inertia torque 1 ($-u\frac{\partial v}{\partial x}$), CONVT2 is the inertia torque 2 ($-v\frac{\partial v}{\partial y}$), PRESSURE is the pressure torque ($-\frac{\partial p}{\partial y}$), VS is the viscous torque ($\mu\nabla^2 v$), and TOTAL is the resultant torque of above torques in the poloidal direction. For the convenience of readability, the torque terms are replaced by force in the above parentheses.

boundary perturbations: below the threshold (nearly locked regime), on the threshold (just locked regime), and above the threshold (strongly locked regime). The resistivity and viscosity are adopted as $\eta = 10^{-4}$ and $\mu = 10^{-3}$.

3.1. *Time-varying boundary perturbation*

The time-varying boundary condition is employed as $\xi = \xi_0 t$, where ξ is the boundary perturbation strength and $\xi_0 = 10^{-6}$. In the previous investigation, i.e. Fitzpatrick (2003), the scalings of error field penetration thresholds are determined by a variety of parameters. The normalized resistivity and viscosity employed in Fitzpatrick (1998) show $R > 1$ ($R = \kappa^{1/5}\tau_H^{1/15}\tau_R^{-1/30}\tau_V^{-1/30}$), which indicates that the Rutherford regime holds. Conventionally, in tokamak plasmas, the most unstable tearing mode is 2/1 or 3/2 mode, thus we may assume $q = rB_\phi/RB_\theta(r) \approx 2$, $r/R \approx 1/4$, $a = 2r_s$, and $\mu(r) = \mu(r_s) = \mu$, where r_s is the rational surface viscosity. Then we obtain $R \approx 1.58$ under the condition that resistivity, $\eta = 10^{-4}$, and viscosity, $\mu = 10^{-3}$. Furthermore, $R > 1$ corresponds to $\mu\eta > 10^{-13}$, and even both normalized resistivity and viscosity are as big as unity. The maximum value of R is only $R \approx 2.7$, which indicates that R cannot be very large. Comparing (59) with (42) in Fitzpatrick (1998), we then obtain,

$$\frac{\hat{\xi}_{\mathrm{Rc}}}{\hat{\xi}_{\mathrm{VRc}}} = \frac{1.167P^{1/3}Q_0R^3}{1.026P^{1/3}Q_0R^{5/2}} = 1.137R^{1/2} \approx 1.43, \tag{4}$$

where$\hat{\xi}_{\mathrm{Rc}}$ and$\hat{\xi}_{\mathrm{VRc}}$ are the normalized critical error field amplitudes in the Rutherford and visco-resistive regimes, respectively.

Here we present an example to describe the time evolutions of the island growth, the poloidal velocity, and various poloidal torques on the rational surface. As shown in Fig. 1(a), the processes may be divided into three stages: before locking, in which the island with low amplitude grows slowly; on locking, where island rises suddenly; and after locking, where the island with high amplitude grows slowly again. It is

https://doi.org/10.1017/S0022377813001384 Published online by Cambridge University Press

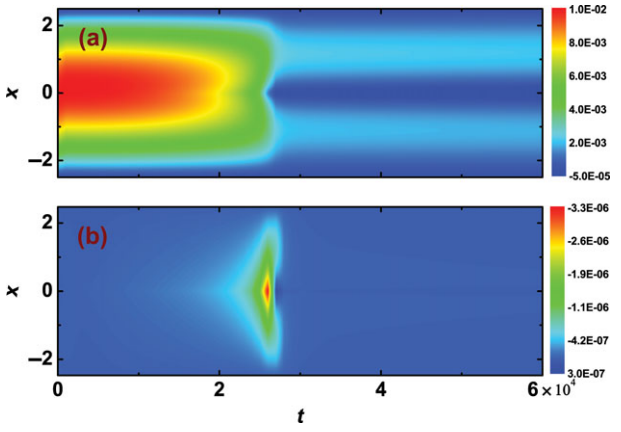


FIGURE 2. (Color online) (a) Time evolution of AAPV, V, distributed in the x-direction (radial direction) with initial velocity, $V_0 = 0.01$, and boundary perturbation value, $\xi = 10^{-6}t$. (b) Time evolution of azimuthally averaged poloidal resultant torque distributed in the x-direction (radial direction).

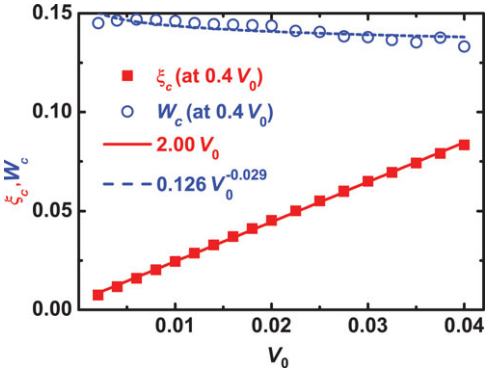


FIGURE 3. (Color online) Critical boundary perturbations, ξ_c, and island widths, W_c, obtained in different initial poloidal velocities, V_0. The symbols represent the data, and the lines are the fit curves.

found by comparing Fig. 1(b) with Fig. 2(b) that the poloidal electromagnetic (EM) and viscous (VS) torques are much larger than others. Note that both EM and VS torques grow slowly before the locking, grow up suddenly once the locking occurs, and finally decrease slowly after the locking. This is a complete process with the time-varying boundary perturbation condition. Furthermore, we find that $|\partial p/\partial y| \gg |v\partial v/\partial y| \gg |u\partial v/\partial x|$, where u is the x-component (radial) and v is the y-component (poloidal) of the velocity.

We then discuss the scaling in the Rutherford and visco-resistive regimes through series of initial velocities and error field-locked mode thresholds. According to the theory (Fitzpatrick 1998) and simulation parameters, the Rutherford regime requires $V_0 \leqslant 0.043$ with locked mode threshold arising at $2/5$ of its initial velocity. The fitted curve of the Rutherford regime is $\xi_c = 2.00\ V_0$ in Fig. 3. The theoretical threshold of visco-resistive regime is $\xi_c = 2.07\ V_0$. Thus, roughly speaking, the scaling of the Rutherford regime approximately equals to the scaling of the visco-resistive regime, which is similar to that in Fitzpatrick (2003) based on parameters under the $R > 1$ condition. Besides, according to the previous analysis, nonlinear stage appears

https://doi.org/10.1017/S0022377813001384 Published online by Cambridge University Press

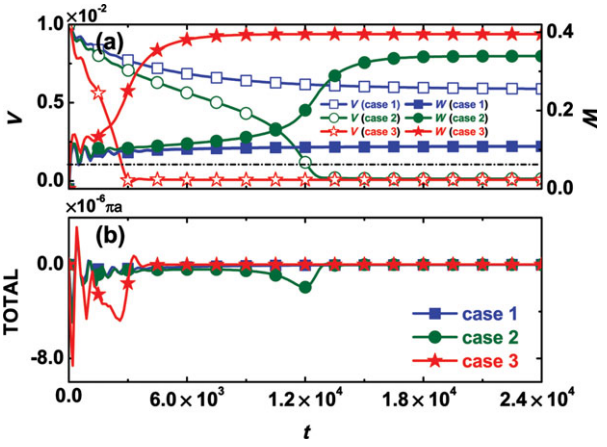


FIGURE 4. (Color online) (a) Time evolution of AAPV, V on the rational surface applied with the identical initial velocity, $V_0 = 0.01$ in three different regimes such as below the threshold (nearly locked regime, case 1), on the threshold (just locked regime, case 2), and above the threshold (strongly locked regime, case 3) denoted by hollow symbol-lines; the solid symbol-lines represent the relevant island width, W, evolution. The horizontal dash-dotted line represents the maximum value of the linear layer width. (b) The corresponding time evolution of the azimuthally averaged poloidal resultant torque on the rational surface (TOTAL).

once the island width exceeds the linear layer width (Rutherford 1973; Fitzpatrick 1993; Fitzpatrick 1998; Kikuchi et al. 2006). The corresponding linear layer of the Rutherford regime is the visco-resistive layer, which is $\delta_{\mathrm{VR}} = \tau_H^{1/3}\tau_R^{-1/6}\tau_V^{-1/6}r_s \approx 0.068r_s$ based on the parameters adopted. Shown in Fig. 3, the nonlinear phase can be easily reached. Thus, above parameters are in the Rutherford regime, corresponding to the previous theoretical analysis (Fitzpatrick 1998). In addition, the dependence of the critical locked island widths on the corresponding velocities matches well with the theoretical result in Fitzpatrick (1998).

Fixed boundary perturbation

The simulation with fixed boundary perturbations can reveal the time evolution of the islands in the Rutherford regime. To better understand the process of the Rutherford regime, we consider three different states: below the threshold (nearly locked regime), on the threshold (just locked regime), and above the threshold (strongly locked regime). Since the island width is larger than the maximum value of the linear layer width, $\delta_{\mathrm{VR}} = \tau_H^{1/3}\tau_R^{-1/6}\tau_V^{-1/6}r_s \approx 0.068r_s$, as shown in Fig. 4(a), all the three states are in the Rutherford regime. It is also indicated in Fig. 4(a) that the island evolutions display oscillation characteristics in the early period, which are similar to the theoretical prediction (Ma et al. 1996; Fitzpatrick 1998). The island is in the low amplitude saturation process in the nearly locked regime, whereas the island grows fast once the rational surface is locked to the island and then saturates with a high amplitude in the strongly locked regime. Meanwhile, the corresponding azimuthally averaged poloidal velocities (AAPVs) and total poloidal torques also oscillate, as shown in Figs. 4(a) and (b). Moreover, it is clear that the oscillating islands are larger than the linear layer width even when they oscillate to the minimum values. It is found by comparing the various poloidal torques in Fig. 4(b) that the resultant torque is mainly composed of EM and VS torques, which are similar to the case

https://doi.org/10.1017/S0022377813001384 Published online by Cambridge University Press

of time-varying boundary perturbations. In addition, AAPV shows similar evolution trend once the error field amplitude exceeds the locked mode threshold.

4. Conclusions

We have numerically investigated the error field penetration process in the magnetic island mode locking by using a two-dimensional resistive MHD model in slab geometry. In the case of the time-varying boundary condition, the time evolutions of islands, flow velocities, and various torques are presented and the various torques on the rational surface are compared. Moreover, it is found that the scaling of the Rutherford regime is similar to that in visco-resistive regime. In the case of the fixed boundary condition, different physical processes in three types of initial states in the Rutherford regimes are illustrated through numerical simulation. Such investigations may apply time-scale estimates for plasma responses to error field correction (EFC) and RMP in tokamak experiments.

Acknowledgements

This work is supported by NMCSFP under grant Nos. 2013GB102000 and 2011GB107000, NSFC under grant Nos. 11275043, 11005015, 10935004, and 11261140326, NCET, and FRFCU (DUT12ZD201).

REFERENCES

Boozer, A. H. 1996 *Phys. Plasmas* **3**, 4620.

Buttery, R. J., De' Benedetti, M., Gates, D. A., Gribov, Y., Hender, T. C., La Haye, R. J., Leahy, P., Leuer, J. A., Morris, A. W., Santagiustina, A., et al. 1999 *Nucl. Fusion* **39**, 1827.

Buttery, R. J., De' Benedetti, M., Hender, T. C. and Tubbing, B. J. D. 2000 *Nucl. Fusion* **40**, 807.

Callen, J. D. 2011 *Nucl. Fusion* **51**, 094026.

Fishpool, G. M. and Haynes, P. S. 1994 *Nucl. Fusion* **34**, 109.

Fitzpatrick, R. 1993 *Nucl. Fusion* **33**, 1049.

Fitzpatrick, R. 1998 *Phys. Plasmas* **5**, 3325.

Fitzpatrick, R. 2003 *Phys. Plasmas* **10**, 1782.

Hender, T. C., Fitzpatrick, R., Morris, A. W., Carolan, P. G., Durst, R. D., Edlington, T., Ferreira, J., Fielding, S. J., Haynes, P. S., Hugill, J., et al. 1992 *Nucl. Fusion* **32**, 2091.

Hender, T. C., Wesley, J. C., Bialek, J., Bondeson, A., Boozer, A. H., Buttery, R. J., Garofalo, A., Goodman, T. P., Granetz, R. S., Gribov, Y., et al. 2007 *Nucl. Fusion* **47**, S128.

Hu, Q. M., Yu, Q., Rao, B., Ding, Y. H., Hu, X. W., Zhuang, G. and the J-TEXT Team 2012 *Nucl. Fusion* **52**, 083011.

Jensen, T. H. and Leonard, A. W. 1991 *Phys. Fluids B* **3**, 3422.

Jin, W., Ding, Y. H., Rao, B., Hu, Q. M., Jin, X. S., Wang, N. C., Zhang, X. Q., Wang, Z. J., Chen, Z. Y., Zhuang, G., et al. 2013 *Plasma Phys. Control. Fusion* **55**, 035010.

Kikuchi, Y., Finken, K. H., Jakubowski, M., Lehnen, M., Reiser, D., Sewell, G., Wolf, R. C. and the TEXTOR team 2006 *Plasma Phys. Control. Fusion* **48**, 169.

Lazzaro, E., Buttery, R. J., Hender, T. C., Zanca, P., Fitzpatrick, R., Bigi, M., Bolzonella, T., Coelho, R., DeBenedetti, M., Nowak, S., et al. 2002 *Phys. Plasmas* **9**, 3906.

Liu, Y., Connor, J. W., Cowley, S. C., Ham, C. J., Hastie, R. J. and Hender, T. C. 2012 *Phys. Plasmas* **19**, 102507.

Ma, Z. W., Wang, X. and Bhattacharjee, A. 1996 *Phys. Plasmas* **3**, 2427.

Mirnov, S., Wesley, J., Fujisawa, N., Gribov, Y., Gruber, O., Hender, T., Ivanov, N., Jardin, S., Lister, J., Perkins, F., et al. 1999 *Nucl. Fusion* **39**, 2251.

Nave, M. F. F. and Wesson, J. A. 1990 *Nucl. Fusion* **30**, 2575.

Parker, R. D. 1992 *Theory of Fusion Plasmas. Proceedings of the Joint Varenna-Lausanne International Workshop*, Varenna, Italy. Bologna, Italy: Editrice Compositori, p. 399.

https://doi.org/10.1017/S0022377813001384 Published online by Cambridge University Press

Rutherford, P. H. 1973 *Phys. Fluids* **16**, 1903.
Waelbroeck, F. L., Joseph, I., Nardon, E., Bécoulet, M. and Fitzpatrick, R. 2012 *Nucl. Fusion* **52**, 074004.
Wang, X. and Bhattacharjee, A. 1997 *Phys. Plasmas* **4**, 748.
Wang, Z. X., Wang, X., Dong, J. Q., Kishimoto, Y. and Li, J. Q. 2008 *Phys. Plasmas* **15**, 082109.
Wang, Z. X., Wang, X. G., Dong, J. Q., Lei, Y. A., Long, Y. X., Mou, Z. Z. and Qu, W. X. 2007 *Phys. Rev. Lett.* **99**, 185004.
Wang, H. H., Wang, Z. X., Wang, X. Q. and Wang, X. G. 2013 *Phys. Plasmas* **20**, 062105.
Wolf, R. C., Biel, W., de Bock, M. F. M., Finken, K. H., Gunter, S., Hogeweij, G. M. D., Jachmich, S., Jakubowski, M. W., Jaspers, R. J. E., Kramer-Flecken, A., et al. 2005 *Nucl. Fusion* **45**, 1700.
Wolfe, S. M., Hutchinson, I. H., Granetz, R. S., Rice, J., Hubbard, A., Lynn, A., Phillips, P., Hender, T. C., Howell, D. F., La Haye, R. J., et al. 2005 *Phys. Plasmas* **12**, 056110.
Xu, T., Hu, Q. M., Hu, X. W. and Yu, Q. Q. 2011 *Chin. Phys. Lett.* **28**, 095202.
Yu, Q., Güenter, S. and Finken, K. H. 2009 *Phys. Plasmas* **16**, 042301.
Yu, Q., Güenter, S., Kikuchi, Y. and Finken, K. H. 2008 *Nucl. Fusion* **48**, 024007.
Zha, X. J., Zhu, S. Z., Yu, Q. Q. and Wang, Y. 2005 *Chin. Phys.* **14**, 2552.

https://doi.org/10.1017/S0022377813001384 Published online by Cambridge University Press